Production, Separation, Isolation, and Spectroscopic Study of Dysprosium Endohedral Metallofullerenes

Nikos Tagmatarchis and Hisanori Shinohara*

Department of Chemistry, Nagoya University, Nagoya 464-8602, Japan

Received June 12, 2000. Revised Manuscript Received August 17, 2000

The first successful production and chromatographic isolation of dysprosium endohedral metallofullerenes are reported. A series of 18 endohedral fullerenes have been separated and isolated having mainly two dysprosium metals engaged in a range of fullerene cages from C_{80} up to C_{94}. All these newly synthesized metallofullerenes are characterized by LD-TOF mass spectrometry and UV−vis−NIR absorption spectroscopy. Their possible molecular symmetry, HOMO−LUMO band gap, and electronic structure are discussed in terms of their absorption spectra and HPLC elution time. Their separation and isolation procedure by multistage high-performance liquid chromatography is discussed in detail.

Introduction

Fullerenes containing metal atoms inside the cage, the so-called endohedral metallofullerenes,[1] are unique materials that possess novel electronic and physical properties.[2−5] One of the most intriguing properties of these materials is that a substantial charge transfer from the entrapped metal atoms to the fullerene cage occurs.[6] Because of the difficulty in producing macroscopic quantities of pure samples, the experimental characterization of metallofullerenes has been hindered.

The arc discharge method of graphite rods discovered in 1990 was a breakthrough to the production of these materials in large quantities.[7,8] Up to now the vast majority of the produced endohedrals is based mainly on Group 3 elements and especially on La,[6,9,10] Y,[11,12] and Sc[11,13] metals. Very little attention has been given on dysprosium metallofullerenes, although the yield of their formation is similar to that of lanthanum ones,[14] which are one of the most extensively studied metallofullerenes.

Although progress in the area is very fast, there are still many unknown subjects such as the growth mechanism of metallofullerenes, how metals are trapped inside the carbon cages, and how the electronic properties and chemical reactivity of hollow fullerenes change upon metal encapsulation. Also, the separation and purification of the metallofullerenes are crucial for further characterization of these materials. However, no systematic studies have been reported on the HPLC (high-performance liquid chromatography) separation of the metallofullerenes.

Here, we report the first systematic study on HPLC separation and isolation of dysprosium endohedral metallofullerenes. Furthermore, we propose that their UV−vis−NIR electronic absorption spectra are useful tools in predicting not only their possible molecular symmetry but also the HOMO−LUMO energy gap and their electronic structure.

Experimental Section

Details for the production of endohedral metallofullerenes are decribed elsewhere.[15] Briefly, soot containing various Dy metallofullerenes was produced by the direct current arc discharge method of Dy_2O_3/graphite composite rods (12.5 × 12.5 × 300 mm, 0.8 wt %, Toyo Tanso Co.). The dysprosium composite rods were heat-treated at a high temperature of 1600 °C. These rod conditions have been found to be crucial for the efficient production of this kind of metallofullerenes via the arc discharge method. The so-produced soot was collected under totally anaerobic conditions to avoid any degradation from air during the collection procedure. Then, it was Soxhlet-extracted first by carbon disulfide and then by pyridine. In general, endohedral monometallofullerenes are more extractable with pyridine than with carbon disulfide in

---

* To whom correspondence should be addressed. E-mail: nori@nano.chem.nagoya-u.ac.jp.

(1) Shinohara, H. *Rep. Prog. Phys.* **2000**, *63*, 843.

(2) Chai, Y.; Guo, C.; Jin, C.; Haufler, R. E.; Chibante, L. P. F.; Fure, J.; Wang, L.; Alford, J. M.; Smalley, R. E. *J. Phys. Chem.* **1991**, *95*, 7564.

(3) Nagase, S.; Kobayashi, K.; Akasaka, T. *Bull. Chem. Soc. Jpn.* **1996**, *69*, 2131.

(4) Akasaka, T.; Nagase, S.; Kobayashi, K.; Walchli, M.; Yamamoto, K.; Funasaka, H.; Kako, M.; Hoshito, T.; Erata, T. *Angew. Chem., Int. Ed. Engl.* **1997**, *36*, 1643.

(5) Sato, W.; Sueki, K.; Kikuchi, K.; Kobayashi, K.; Suzuki, S.; Achiba, Y.; Nakahara, H.; Ohkuba, Y.; Ambe, F.; Asai, K. *Phys. Rev. Lett.* **1998**, *80*, 133.

(6) Yamamoto, K.; Funasaka, H.; Takahashi, T. *J. Phys. Chem.* **1994**, *98*, 2008.

(7) Kratschmer, W.; Lamb, L. D.; Fostiropoulos, K.; Huffman, D. R. *Nature* **1990**, *347*, 354.

(8) Haufler, R. E.; Conceicao, J.; Chibante, L. P. F.; Chai, Y.; Byrne, N. E.; Flanagan, S.; Haley, M. M.; O'Brien, S. C.; Pan, C.; Xiao, Z.; Billups, W. E.; Ciufolini, M. A.; Hauge, R. H.; Margrave, J. L.; Wilson, L. J.; Curl, R. F.; Smalley, R. E. *J. Phys. Chem.* **1990**, *94*, 8634.

(9) Johnson, R. D.; de Vries, M. S.; Salem, J. R.; Bethune, D. S.; Yannoni, C. S. *Nature* **1992**, *355*, 239.

(10) Kikuchi, K.; Suzuki, S.; Nakao, Y.; Nakahara, N.; Wakabayashi, T.; Shiromaru, H.; Saito, K.; Ikemoto, I.; Achiba, Y. *Chem. Phys. Lett.* **1993**, *216*, 67.

(11) Shinohara, H.; Sato, H.; Saito, Y.; Ohkohchi, M.; Ando, Y. *J. Phys. Chem.* **1992**, *96*, 3571.

(12) Weaver, J. H.; Chai, Y.; Kroll, G. H.; Jin, C.; Ohno, T. R.; Haufler, R. E.; Guo, T.; Alford, J. M.; Conceicao, J.; Chibante, L. P. F.; Jain, A.; Palmer, G.; Smalley, R. E. *Chem. Phys. Lett.* **1992**, *190*, 460.

(13) Yannoni, C. S.; Hoinkis, M.; de Vries, M. S.; Bethune, D. S.; Salem, J. R.; Crowder, M. S.; Johnson, R. D. *Science* **1992**, *256*, 1191.

(14) Huang, H.; Yang, S. *J. Phys. Chem.* **1998**, *102*, 10196.

(15) Shinohara, H.; Takata, M.; Sakata, M.; Hashizume, T.; Sakurai, T. *Mater. Sci. Forum.* **1996**, *232*, 207.

10.1021/cm000476h CCC: $19.00

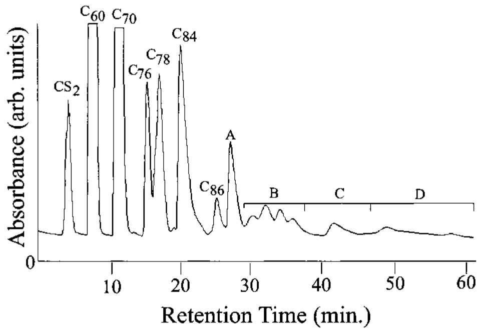

Figure 1. HPLC profile of a carbon disulfide extract of the soot containing dysprosium metallofullerenes with a 5PYE column. Regions A, B, C, and D contain dysprosium metallofullerenes and are subjected to further separation (see text and Supporting Information for HPLC final separation).

which hollow fullerenes and dimetal endohedral fullerenes are most abundant.

HPLC (LC-908-C60, Japan Analytical Industry) was performed for the separation of dysprosium endohedrals using a Buckyprep (20 × 250 mm, Nakalai Tesque), a 5PYE (20 × 250 mm, Nakalai Tesque), and a Buckyclutcher (20 × 300 mm, Regis Chemical) columns.

The purity of the newly synthesized materials (>99%) was confirmed by both positive and negative laser-desorption time-of-flight (LD-TOF) mass spectrometry.

The UV–vis–NIR spectra of the isolated dysprosium metallofullerenes were recorded between 400 and 2000 nm in carbon disulfide solutions by using a Shimadzu UV-3101PC spectrophotometer.

Results and Discussion

1. Separation and Isolation of Dysprosium Metallofullerenes. Each dysprosium metallofullerene was separated and isolated from various hollow fullerenes in isomer free forms by a multistage HPLC procedure. In the first HPLC stage, dysprosium-containing metallofullerenes were roughly separated from empty higher fullerenes up to C_{86} by using a 5PYE column (15 mL/min flow rate, toluene eluent). After C_{86} the chromatogram (Figure 1) was divided into four regions, A, B, C, and D, and each region was analyzed separately.

Region A contains Dy@C_{82} (I)[16–18] along with Dy_2@C_{84} (I) and has the shortest retention time among the whole series of dysprosium endohedral metallofullerenes. Their separation was achieved on a Buckyclutcher column (10 mL/min flow rate, toluene eluent) (see Supporting Information).

Region B, which contains the hollow fullerenes from C_{88} to C_{92}, was injected into a Buckyclytcher column (10 mL/min flow rate, toluene eluent). With this column we were able to separate and remove empty higher fullerenes that elute earlier than metallofullerenes. The fraction of metallofullerenes was further separated by a recycling HPLC on a Buckyprep column (15 mL/min flow rate, toluene eluent). After three cycles we managed to isolate four fractions of metallofullrenes, that is, E, F, G, and H (Figure 2). Each of these fractions was then re-injected into a Buckyclutcher column for the final purification. We, therefore, managed to isolate Dy@C_{82} (I) from fraction E, Dy_2@C_{86} (I) and Dy_2@C_{82} (I) from fraction F, Dy_2@C_{84} (II) from fraction G, and Dy_2@C_{84} (III) from fraction H (see Supporting Information).

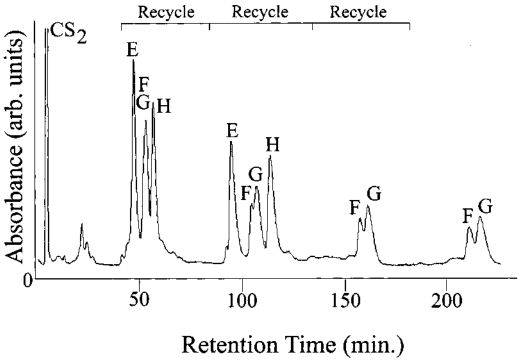

Figure 2. Recycling HPLC profile of region B with a Buckyprep column, after the removal of empty higher fullerenes C_{88}–C_{92}.

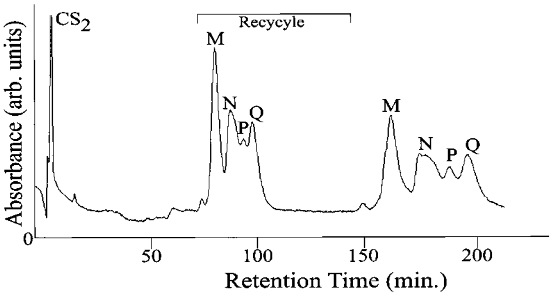

Figure 3. Recycling HPLC profile of region D with a Buckyprep column, after the removal of empty higher fullerenes C_{96} and C_{98}.

A similar isolation procedure was followed for the rest of the main regions C and D. Region C, which contains the C_{94} fullerene, was injected into the Buckyclutcer column to separate it from the metallofullerenes that coelute. There are two major metallofullerene fractions K and L (see Supporting Information). Fraction L contains a single isomer of Dy_2@C_{88} (I). Fraction K was introduced into the Buckyprep column and after recycling for 3 h the fraction was resolved into two isomers of Dy_2@C_{90} (I) and Dy_2@C_{90} (II) (see Supporting Information). Although Dy_2@C_{88} (I) is smaller in size than Dy_2@C_{90} (I) and Dy_2@C_{90} (II), it elutes later. Recent studies have shown a correlation between the HPLC retention time and the molecular geometry of fullerenes.[19] Generally, a spherical-shaped fullerene has a shorter retention time than that of an elongated one. Hence, we can expect that the molecular geometry of Dy_2@C_{88} (I) should be somehow more elliptical while Dy_2@C_{90} (I) and Dy_2@C_{90} (II) should be spherical in geometry.

Finally, region D, which contains the higher empty fullerenes, C_{96} and C_{98}, was injected into the Buckyclutcher column to remove the hollow fullerenes. The fraction that contains the metallofullerenes was once again injected into Buckypep and recycled for more than 3 h to resolve four different fractions, that is, M, N, P, and Q (Figure 3). Fraction Q is a single compound of Dy_2@C_{92} (III). Re-injection and recycling of fraction M

---

(16) Ding, J.; Yang, S. *J. Phys. Chem. Solids* **1997**, *58*, 1661.

(17) Gu, G.; Huang, H.; Yang, S.; Yu, P.; Fu, J.; Wong, K. L. G.; Wan, X.; Dong, J.; Du, Y. *Chem. Phys. Lett.* **1998**, *289*, 167.

(18) Huang, H.; Yang, S.; Zhang, X. *J. Phys. Chem. B* **2000**, *104*, 1473.

(19) Wan, T. S. M.; Zhang, H. W.; Nakane, T.; Xu, Z. D.; Inakuma, M.; Shinohara, H.; Kobayashi, K.; Nagase, S. *J. Am. Chem. Soc.* **1998**, *120*, 6806.

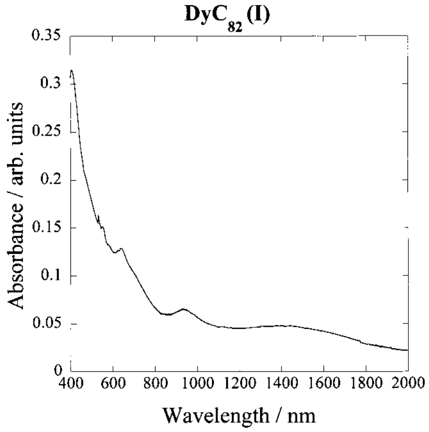

Figure 4. UV−vis−NIR absorption spectrum of the isolated Dy@C_{82} (I) in carbon disulfide.

on Buckyprep for 4 h separates three different metallofullerenes (see Supporting Information), namely, Dy_2@C_{86} (II), Dy_2@C_{88} (II), and Dy_2@C_{92} (I) in order of increasing retention time. Similarly, recycling of fraction N on Buckyprep resolves two new dysprosium metallofullerenes, Dy_2@C_{90} (III) and Dy_2@C_{94} (I) (see Supporting Information). As described before, we expect that the isomers Dy_2@C_{86} (II), Dy_2@C_{88} (II), and Dy_2@C_{90} (III) should have an elongated shape as they elute considerably later than their other isomers. Eventually, recycling of fraction P on the Buckyclutcher column separates Dy_2@C_{94} (II) and Dy_2@C_{92} (II) (see Supporting Information). Interestingly, the only endohedral metallofullerenes extracted by pyridine were Dy@C_{82} (I) and Dy_2@C_{80} (I). Although the former is the most abundant dysprosium metallofullerene found extractable in both carbon disulfide and pyridine, the latter was only extractable in pyridine in low abundance. However, as long as it was extracted from the soot by pyridine, it readily became soluble not only in carbon disulfide but also in toluene. In addition, the fact that apart from Dy@C_{82} (I) the only dysprosium metallofullerenes isolated so far were didysprosium fullerenes supports the idea that this metal could aggregate mostly as dimer species upon the formation of the endohedrals.

We have, therefore, managed to produce, separate, and isolate in isomer pure form the total number of 18 different dysprosium endohedral metallofullerenes, that is, Dy@C_{82} (I), Dy_2@C_{80} (I), Dy_2@C_{82} (I), Dy_2@C_{84} (I), Dy_2@C_{84} (II), Dy_2@C_{84} (III), Dy_2@C_{86} (I), Dy_2@C_{86} (II), Dy_2@C_{88} (I), Dy_2@C_{88} (II), Dy_2@C_{90} (I), Dy_2@C_{90} (II), Dy_2@C_{90} (III), Dy_2@C_{92} (I), Dy_2@C_{92} (II), Dy_2@C_{92} (III), Dy_2@C_{94} (I), and Dy_2@C_{94} (II). Their UV−vis−NIR spectra were recorded and the results are discussed below.

2. UV−Vis−NIR Absorption Spectroscopy. The electronic absorption spectrum of the isolated Dy@C_{82} (I) shows characteristic absorption bands at 555, 640, 937, and 1410 nm while the onset of the spectrum continues down to 1800 nm (Figure 4). This is a typical absorption spectrum of a M@C_{82} type of metallofullerenes having Group 3 metal atoms inside (e.g., Y@C_{82}, Gd@C_{82}, La@C_{82}, etc.). The absorption peaks are slightly blue-shifted relative to those of La@C_{82} and Y@C_{82}. The *f*−*f* transitions of the metal atom are not observed presumably due to masking of the broad absorption band of the cage. As it is well-known that in M@C_{82} (M= La, Y, Gd, etc.) the metal atoms are in the 3+ oxidation state, we also expect that Dy should also transfer three electrons to the fullerene cage because of the similarity in the absorption spectra. We attribute the broad absorption profile down to 1800 nm to an open-shell electronic structure with a low molecular symmetry—probably either C_{2v} or C_{3v} or C_2 analogous to the hollow higher fullerene C_{82}. This would lead to a half-filled molecular orbital configuration on the fullerene cage.

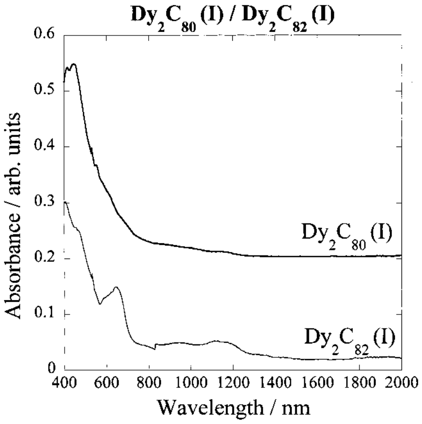

Figure 5. UV−vis−NIR absorption spectra of the isolated Dy_2@C_{80} (I) and Dy_2@C_{82} (I) in carbon disulfide.

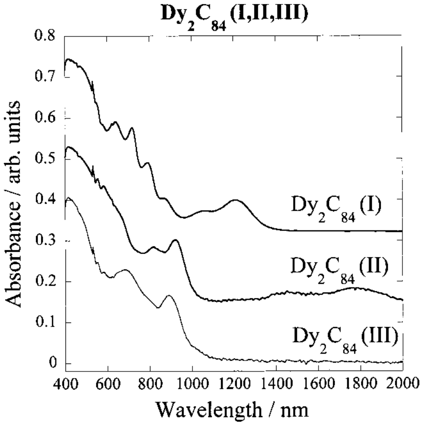

Figure 6. UV−vis−NIR absorption spectra of the isolated Dy_2@C_{84} (I), Dy_2@C_{84} (II), and Dy_2@C_{84} (III) in carbon disulfide.

Figure 5 shows the UV−vis−NIR spectra of Dy_2@C_{80} (I) and Dy_2@C_{82} (I). The salient features for Dy_2@C_{82} (I) are at 644, 946, and 1137 nm. The onset of the spectrum is at 1510 nm. Basically, the onset of the UV−vis−NIR spectrum corresponds to the lowest electronic transitions and thus is a good measure for the HOMO−LUMO energy gap of fullerenes. Again, because of the red shift of the absorption onset (relative to hollow fullerenes), the HOMO−LUMO band gap of Dy_2@C_{82} (I) should be smaller than that of the corresponding hollow fullerene. For Dy_2@C_{80} (I) only weak absorptions are seen at 600, 688, and 1133 nm.

The absorption spectra for the three isomers of Dy_2@C_{84} (I), Dy_2@C_{84} (II), and Dy_2@C_{84} (III) are presented in Figure 6. These materials have the highest abundance among the isolated didysprosium metallofullerenes. The overall spectral features are different from each other. The spectrum of the first isomer shows pronounced absorptions at 635, 715, 790, 880, 1035, and 1208 nm. The onset goes down at around 1450 nm and

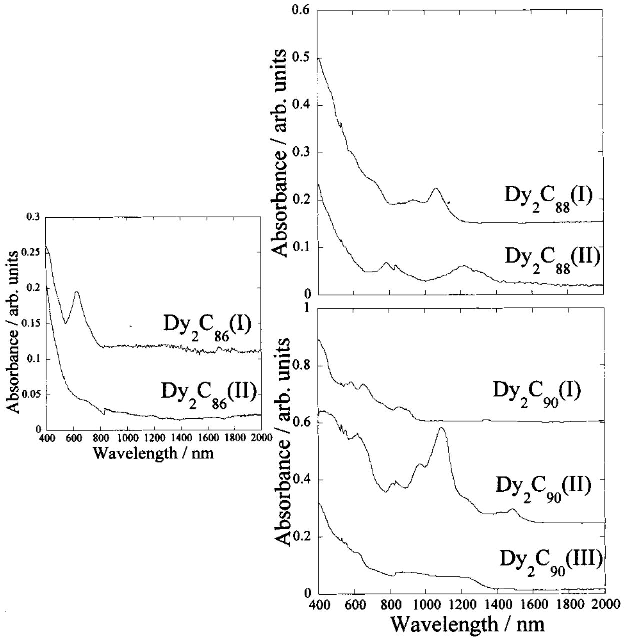

Figure 7. UV–vis–NIR absorption spectra of the isolated Dy$_2$@C$_{86}$ (I) and Dy$_2$@C$_{86}$ (II), Dy$_2$@C$_{88}$ (I) and Dy$_2$@C$_{88}$ (II), and Dy$_2$@C$_{90}$ (I), Dy$_2$@C$_{90}$ (II), and Dy$_2$@C$_{90}$ (III) in carbon disulfide.

overall the spectrum is similar to that of the first isomer of Sc$_2$@C$_{84}$ (I).[20] The spectrum of the second isomer Dy$_2$@C$_{84}$ (II) has similar features to that of Sc$_2$@C$_{84}$ (II),[20] that is, four absorptions at 813, 920, 1453, and 1782 nm while the onset of the spectrum lies down at 2000 nm. This is characteristic to metallofullerenes with open-shell electronic structures, indicating a very small HOMO–LUMO energy gap. The spectrum of the third isomer Dy$_2$@C$_{84}$ (III), similar to that of Sc$_2$@C$_{84}$ (III),[20] is less rich, showing absorption bands at 675 and 889 nm only. The absorption onset is at 1100 nm, consistent with the experimental observation of its slightly higher yield of production. The strong similarities of the electronic spectra with those of three discandium metallofullerenes having the known symmetries of C_s, C_{2v}, and D_{2d} give evidence for their expected molecular geometries. We presume that Dy$_2$@C$_{84}$ (I), Dy$_2$@C$_{84}$ (II), and Dy$_2$@C$_{84}$ (III) have C_s, C_{2v}, and D_{2d} molecular symmetries, respectively.

Figure 7 presents the absorption spectra of Dy$_2$@C$_{86}$ (I) and Dy$_2$@C$_{86}$ (II), Dy$_2$@C$_{88}$ (I) and Dy$_2$@C$_{88}$ (II), and the three isomers of Dy$_2$@C$_{90}$ (I), Dy$_2$@C$_{90}$ (II), and Dy$_2$@C$_{90}$ (III), respectively. The two isomers of Dy$_2$@C$_{86}$ (I) and Dy$_2$@C$_{86}$ (II) are the least abundant together with Dy$_2$@C$_{80}$ (I). Both spectra are featureless with only a strong absorption for the first isomer at 631 nm and a broad band that starts at 900 and continues down to 1600 nm. The onset for the second isomer is at 1400 nm. For Dy$_2$@C$_{88}$ (I) there are four weak absorptions at 551, 600, 706, and 853 and two stronger ones at 930 and 1060 nm. The onset of the spectrum lies at 1200 nm. In contrast, the second isomer Dy$_2$@C$_{88}$ (II) shows two characteristic absorptions at 782 and 835 nm and a broad band with a maximum at 1210 nm. This difference of the spectra can be attributed to a different symmetry cage that the metals share in the two isomers. Again, the observed large red shift of the absorption onset (with respect to the hollow cages) stems from a smaller HOMO–LUMO energy gap. Interestingly, the spectrum of the isomer Dy$_2$@C$_{90}$ (II) is very rich in features, showing strong absorption bands at 617, 813, 840, 970, 1090, 1413, and 1490 nm. The onset of the spectrum is at 1670 nm, which is very red shifted with respect to the other two isomers, indicating a smaller HOMO–LUMO energy gap. These features can be ascribed to the encapsulation of dysprosium metal atoms in a high-symmetry fullerene network.

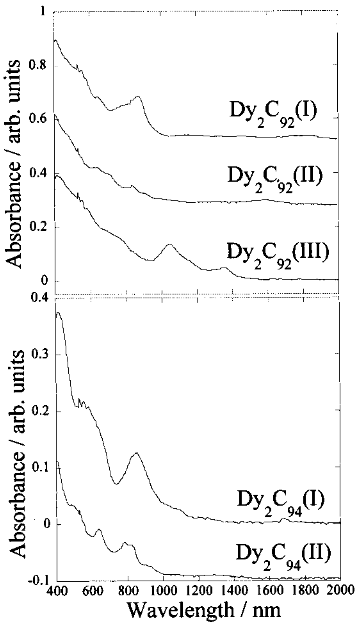

Figure 8. UV–vis–NIR absorption spectra of the isolated Dy$_2$@C$_{92}$ (I), Dy$_2$@C$_{92}$ (II), and Dy$_2$@C$_{92}$ (III) and Dy$_2$@C$_{94}$ (I) and Dy$_2$@C$_{94}$ (II) in carbon disulfide.

Finally, Figure 8 shows the UV–vis–NIR spectra of the three isomers of Dy$_2$@C$_{92}$ (I), Dy$_2$@C$_{92}$ (II), Dy$_2$@C$_{92}$ (III), and the two isomers of Dy$_2$@C$_{94}$ (I) and Dy$_2$@C$_{94}$ (II), respectively. As the fullerene cage becomes larger, the number of structural isomers increases and the molecular symmetry of the system is reduced. This is most likely the case for endohedrals having metal atoms encaged in higher fullerene networks. Their spectra have many characteristic features that appear at similar wavelengths, albeit with different relative intensities.

The electronic absorption spectra of all these newly synthesized metallofullerenes provide further evidence for the number of electron transfers from the encaged metal atom to the fullerene cages. The observed similarity in the absorption spectra to those of Group 3 metallofullerenes suggests that each dysprosium metal atoms donates approximately three electrons to the fullerene cage. Thus, we can expect that didysprosium metallofullerenes are diamagnetic. This diamagnetic behavior of Dy$_2{}^{3+}$@C$_{2n}{}^{6-}$ ($2n = 80, 82, 84, 86, 88, 90, 92, 94$) will allow us to determine their molecular symmetry and correspondingly their isomer structures by high-resolution ^{13}C NMR. These measurements are currently underway in our laboratories and the results will be published elsewhere.

In summary, we have managed to separate and isolate 18 different dysprosium metallofullerenes along

---

(20) Inakuma, M.; Yamamoto, E.; Kai, T.; Wang, C.-R.; Tomiyama, T.; Shinohara, H.; Dennis, T. J. S.; Hulman, M.; Krause, M.; Kuzmany, H. *J. Phys. Chem. B* **2000**, *104*, 5072.

with their structural isomers using the technique of recycling high-performance liquid chromatography. UV–vis–NIR absorption spectra revealed their electronic structure and gave valuable information on their probable molecular symmetry as well as their HOMO–LUMO energy gap.

Acknowledgment. N.T. thanks the Japan Society for the Promotion of Science (JSPS) for the Postdoctoral Fellowship for Foreigner Researchers. H.S. thanks JSPS for the Future Program on New Carbon Nanomaterials.

Supporting Information Available: Recycling HPLC profiles of Fractions E, K, M, N, and P, separation of Dr@C_{82} (I), and HPLC profile of region C. This material is available free of charge via the Internet at http://pubs.acs.org.

CM000476H